Int. J. Morphol.,
43(1):250-257, 2025.

Effect of Different Doses of Celecoxib on the Expression of Basic Fibroblast Growth Factor and Matrix Metalloproteinase-13 as Morphological Indicators in Rat Model of Lumbar Disc Degeneration

Efecto de Diferentes Dosis de Celecoxib en la Expresión del Factor de Crecimiento Básico de Fibroblastos y la Metaloproteinasa de Matriz-13 como Indicadores Morfológicos en un Modelo de Rata de Degeneración del Disco Lumbar

Kejun Hu[1]; Haoran Gao[1] & Xueli Wang[2]

HU, K.; GAO, H. & WANG, X. Effect of different doses of Celecoxib on the expression of basic fibroblast growth factor and matrix metalloproteinase-13 as morphological indicators in rat model of lumbar disc degeneration. *Int. J. Morphol., 43(1)*:250-257, 2025.

SUMMARY: The objective of this study was to investigate the outcomes of various doses of celecoxib (Cel) on the expression of basic fibroblast growth factor (bFGF) and matrix metalloproteinase-13 (MMP-13) in rat model of intervertebral disc degeneration (IVDD) and their correlation. The rat model of IVDD was established, and 68 successfully modeled rats were grouped: A, B, C, and D groups (AG, BG, CG, DG), with 17 rats in each. Pathological changes of the nucleus pulposus (NP) tissue and the expression of bFGF and MMP-13 were detected using hematoxylin-eosin (HE) staining, immunohistochemistry, and Western blotting (WB), followed by Pearson correlation analysis (PCA). HE staining suggested that the degeneration of the NP tissue in BG was clear, and CG and DG slowed down the pathological changes to some extent. The results of immunohistochemistry and WB analysis indicated that the expression of bFGF and MMP-13 in BG was markedly higher as against AG, and the expression in the CG and DG was markedly reduced (P <0.05). The correlation coefficient of bFGF and MMP-13 in immunohistochemical analysis was r=0.981 (P <0.001), and in WB analysis, it was r=0.813 (P <0.001). Cel was found to effectively inhibit the expression of bFGF and MMP-13 during the process of IVDD, slow down the degenerative process, and suggested potential therapeutic effects.

KEY WORDS: Cel; Lumbar disc degeneration; bFGF; MMP-13; Correlation analysis.

INTRODUCTION

Lumbar intervertebral disc nucleus pulposus degeneration refers to the degenerative changes in the NP of the lumbar intervertebral disc (IVD), which is a common spinal disease. The NP is located in the center of the IVD and is rich in water and gelatinous substances, mainly composed of water, collagen, and proteoglycans (Sun *et al*., 2022; Li *et al*., 2024). Its main function is to absorb and disperse spinal load, maintaining the flexibility of the spine. The annulus fibrosus (AF) surrounds the outer layer of the NP and is mainly composed of collagen fibers, providing structural support and stability to the IVD. The cartilage endplate connects the IVD with adjacent vertebral bodies and participates in the transport of nutrients. Long term mechanical stress and improper posture can lead to degeneration of the NP (Zhu *et al*., 2022; Liu & Li, 2022). As age increases, the water and proteoglycan content in the NP decreases, which can also lead to a decrease in its elasticity and ability to absorb impact. In addition, certain genetic factors may increase the risk of IVDD. Other factors including smoking, obesity, malnutrition, and trauma may also accelerate IVDD. During the process of degeneration, the water content in the NP gradually decreases, leading to a reduction in its volume and elasticity. The imbalance of degradation and synthesis of proteoglycans and collagen affects the structure and function of the NP (Kirnaz *et al*., 2022; Xu *et al*., 2023). The apoptosis of NP cells increases, and the activity of MMP increases, leading to the degradation of NP matrix. Along with the inflammatory response, the released inflammatory mediators further damage the IVD tissue. IVDD can lead to disc herniation or rupture, compressing surrounding nerve roots, causing back pain and sciatica, which are the most common symptoms of lumbar

[1]Department of Spine Surgery, Xi'an Hospital of Traditional Chinese Medicine, Xi'an, Shaanxi, Pople' Republic of China.
[2]Department of Radiology, The First Affiliated Hospital of Xi'an Medical University, Xi'an, 710077, Shaanxi Province, China.

Received:2024-09-26 Accepted: 2024-10-24

disc degeneration (Bouhsina *et al*., 2023; Xu *et al*., 2020). It can also lead to a decrease in IVD height, rupture of the AF, affect the stability of the spine, and may cause instability and slippage of the spine. Degenerated IVD is unable to effectively absorb and distribute loads, increasing the burden on adjacent vertebrae and joints, which may lead to further degenerative changes in the spine (Kim *et al*., 2022; Ma *et al*., 2024).

bFGF is an important growth factor that promotes cell proliferation, matrix synthesis, and tissue repair in IVD NP tissue (Chang *et al*., 2020; Liu & Tang, 2023). It can stimulate NP cells to produce collagen and proteoglycans, helping to maintain the structure and function of IVD. Although bFGF has a positive effect on tissue repair, overexpression may lead to matrix degradation and damage to IVD structure, thereby promoting IVDD (Payet *et al*., 2023; Wang *et al*., 2024; James *et al*., 2024). MMP-13 is a protease that can degrade collagen and other matrix components. It is active in the process of IVDD, weakening the structural integrity of the IVD by decomposing matrix components. Overexpression of MMP-13 accelerates the degradation of the NP matrix, leading to IVDD and functional loss (Hu*et al*., 2022; Rabie *et al*., 2023). Cel is a nonsteroidal anti-inflammatory drug (NSAID) that is a selective COX-2 inhibitor. It exerts anti-inflammatory, analgesic, and antipyretic effects by suppressing the activity of COX-2 enzyme and reducing the production of prostaglandins (Antonen *et al*., 2022). By selectively suppressing COX-2 enzyme, Cel reduces the synthesis of inflammatory mediators such as prostaglandins, alleviates inflammatory reactions and related symptoms, and may help alleviate inflammation and pain caused by IVDD. It may also indirectly slow down the degradation process of IVD matrix and protect IVD tissue (Liu *et al*., 2019a; Kasamkattil *et al*., 2023). In summary, the expression and role of bFGF and MMP-13 in the NP tissue of the IVD are of obvious importance for understanding the mechanism of IVDD. Cel, as a NSAID, may play a certain auxiliary role in alleviating the symptoms of IVDD through its anti-inflammatory and analgesic effects. This article aimed to explore the regulatory effects of various doses of Cel on bFGF and MMP-13, with the hope of providing new ideas and potential drug targets for the treatment of IVDD.

MATERIAL AND METHOD

Selection of experimental animals, materials, and equipment

In this experiment, 75 male Sprague-Dawley rats, weighing between 300 - 400 g, were selected and purchased from The First Affiliated Hospital of Xi'an Medical University Animal Center. All rats were housed at The First Affiliated Hospital of Xi'an Medical University Experimental Center under standard conditions, with the room temperature maintained at 25 °C and the relative humidity controlled between 40 % - 70 %. The Cel capsules used in the experiment (0.2 g * 30 capsules, H20203297) were provided by CSPC Ouyi Pharmaceutical Co., Ltd.

The main reagents, materials, and equipment used in the experiment are as follows: Electron microscope (VHX-X1, Keyence (China) Co., Ltd.); Pathological paraffin embedding machine (BK-TEI, Boke Group); Microtome (CM1520, Leica Biosystems (China)); Automatic stainer (HistoCore CHROMAX ST, Leica Biosystems (China)); Vortex mixer (15920D, Thermo Fisher); Electric heating constant temperature water bath (HH-US, Jiangsu Xinchunlan Scientific Instrument Co., Ltd.); Low-temperature refrigerator (TDE30086FV-ULTS, Thermo Fisher); UV-Vis Spectrophotometer (DR6000, Hach Water Quality Analysis Instruments (Shanghai) Co., Ltd.); Gel imaging system (Invitrogen iBright, Thermo Fisher); High-speed low-temperature centrifuge (Allegra C-34R, Beckman Coulter Trading (China) Co., Ltd.); SDS-PAGE electrophoresis apparatus (1658001, Bio-Rad, USA); Rabbit anti-rat bFGF polyclonal antibody (Ab) (K11013-TYZ, Beijing Baiao Laibo Technology Co., Ltd.); Rabbit anti-rat MMP-13 polyclonal Ab (LS-C88705, LSBio); SABC immunohistochemistry kit (QN1229, Beijing Baiao Laibo Technology Co., Ltd.); DAB chromogenic reagent (DA1010, Solarbio); Horseradish peroxidase-labeled goat anti-rabbit IgG (Amyjet Technology Co., Ltd.); Cell lysis buffer (B7435, Merck Sigma-Aldrich); PMSF (P7626, Merck Sigma-Aldrich); Ammonium persulfate (7727-54-0, Merck Sigma-Aldrich); Concentrated b-actin Ab (bs-0061R, Bioss); BCA protein assay kit (ml095490, Shanghai Enzyme-Linked Biotechnology Co., Ltd.); ECL kit (PH0353, Phygene Scientific Reagent).

Rat model establishment and grouping

Rats were anesthetized by intraperitoneal injection of 10 % chloral hydrate (3.5 mL/kg). The rats were fixed on the operating table with their abdomens facing up to maintain a good surgical field of view. Under sterile conditions, an approximately 2 cm incision was made along the dorsal midline of the rat, and the skin and muscles were sequentially cut to expose the spinous processes and laminae of the lumbar vertebrae. An 18-gauge needle was inserted and rotated several times at the IVD level (L4/5) to destroy the AF and induce degeneration. The needle was inserted to a depth of 2-3 mm, maintained for 10-20 s, and then withdrawn. After the operation, the muscular and cutaneous layers were stitched sequentially, and the incision was disinfected. Penicillin (100,000 units) was immediately injected

postoperatively to prevent infection. Pain relief medications such as ibuprofen could be used to alleviate postoperative pain in rats. The rats were returned to their cages to observe postoperative recovery, and their diet, activity, and excretion were recorded.

Out of the 75 experimental rats, the IVDD model was successfully established in 68 rats. Three rats failed to be anesthetized during anesthesia, making the operation impossible. Two rats had severe bleeding during the surgical operation, making it impossible to continue the surgery. Two rats failed to wake up successfully postoperatively, possibly due to excessive anesthesia or excessive surgical trauma.

Drug treatment began two weeks after the operation, with the specific grouping and treatment methods as follows.

(1) AG: 17 rats, no treatment was performed.
(2) BG: 17 rats, only physiological saline was given.
(3) CG: 17 rats were orally administered by gavage once daily (30 mg/kg), and intervention time was 3 weeks.
(4) DG: 17 rats were orally administered by gavage once daily (15 mg/kg), and intervention time was 3 weeks.

The experiment lasted for 3 months, and each month, 6 rats were randomly selected from the four groups. After anesthesia, IVD tissue samples were taken for various experimental analyses to assess the effects of Cel on IVDD and therapeutic effects at various doses.

Specimen processing and HE staining

After fixing the rat IVD tissue in 4 % paraformaldehyde solution at 4 °C for 24 h, the tissue was dehydrated and paraffin-embedded to prepare 4 mm thick sections for HE staining, and immunohistochemical experiments for bFGF and MMP-13. The sections were left to stand overnight at 60 °C, and the tissue samples required for WB experiments were stored in a low-temperature freezer at -80 °C. The sections were soaked in xylene solution for 10 min, and then soaked in xylene solution for 5 min. They were moved to anhydrous ethanol I for 1 min, followed by anhydrous ethanol II for 1 min. They were soaked in 80 % alcohol solution for 30 s, then in 70 % alcohol solution for 30 s, and then rinsed with water on three occasions. Subsequently, they were immersed in hematoxylin solution for staining for 5 min, followed by rinsing with water on three occasions. They were differentiated in hydrochloric acid alcohol solution for 5 - 10 s, then rinsed with water twice. Then, they were placed in ammonia water solution for 1-2 min, followed by rinsing with water twice. Subsequently, they were placed in eosin solution for staining for 1 min, followed by rinsing with water twice. Next, they were soaked in 80 % alcohol and 95 % alcohol solutions for 30 s each, then in anhydrous ethanol I for 1 min, and then in anhydrous ethanol II for 2 min. Finally, they were soaked in xylene I for 2 min, followed by soaking in xylene II for 2 min, and then sealed.

Immunohistochemical staining and image processing

The paraffin sections were deparaffinized in xylene in sequence, followed by immersion in 100 % anhydrous ethanol for 2 min, repeated twice. Subsequently, they were dehydrated using graded ethanol, then rinsed in distilled water on three occasions for 3 min each time. They were subjected to treatment with 3 % hydrogen peroxide at 25 °C for a duration of 10 min for inactivating the endogenous enzymes, followed by another round of rinsing. The pH 6.0 citrate buffer was heated to boiling, and the staining rack with the slides was placed in a pressure cooker, timed for 2 min after steaming, then cooled to 25 °C and removed, and washed twice with PBS. Afterwards, 5 % BSA blocking solution was applied, incubation at 25 °C for 20 min, with excess liquid decanted. The first Ab was added to the slides, incubation at 37 °C overnight. The following day, the slides were washed on three occasions with PBS for 3 min each. Then, biotinylated goat anti-rabbit IgG was applied, incubation at 25 °C for 30 min, followed by three washes with PBS. The SABC reagent was applied, and after incubation at 25 °C for 30 min, the slides were washed with PBS, 3 min each time, for a total of four times. The slides were then visualized using DAB chromogen, and the staining process was monitored under a microscope, with staining termination at the appropriate time, followed by counterstaining with hematoxylin. The HE-stained sections and immunohistochemical sections at 200× magnification were observed using a light microscope, and five random high-power fields were selected to quantitatively analyze the integrated optical density (IOD) using Image J software, with the average value of each sample taken as the staining intensity.

WB detection method

100 mg of tissue was mixed with 1 mL of IP lysis buffer and PMSF, homogenized on ice, and after standing for 10 min, centrifuged at 4 °C at 12,000xg for collecting the upper liquid. The BCA method was used to determine protein concentration: Reagent A was combined with Reagent B in a 50:1 ratio for the preparation of the BCA working solution (WS). Both the extracted protein samples and the standards were then diluted using PBS to a volume of 250 μL, mixed with 2.5 mL of BCA WS, and incubated at 25 °C for 2 h. The absorbance was measured at 450 nm, and the protein concentration was determined based on the standard curve. The sample protein concentration was adjusted to 10 mg/mL for later use.

WB experiment and image processing

After wiping the glass, the electrophoresis cell was assembled, and 10 % separating gel and 5 % stacking gel were prepared, with TEMED and APS added to promote polymerization. After the gel solidified, the stacking gel was added, and a comb was inserted. The protein samples to be tested were mixed with loading buffer, and 3 min after boiling, they were added to the wells of the samples, at 80V for 40 min and 120V for 80 min. After electrotransfer to the nitrocellulose membrane, it was blocked with 5 % skim milk solution, and the first Ab (bFGF, MMP-13, or b-actin) were added, incubation overnight at 4 °C. The next day, the secondary Ab were applied, and the incubation continued at 25 °C for 2 h. After chemiluminescence development, the membrane was exposed using X-ray film. Image analysis was performed using a gel image analysis system, with results expressed as the product of net area and average density.

Statistical analysis

Experimental data were presented as mean ± sd and analyzed using SPSS 27.0 software. The SNK-q test was adopted for contrast. The immunohistochemical and WB results of MMP-13 and bFGF in BG were assessed by PCA.

RESULTS

Light microscopy observation results for HE staining

(1) AG: No clear changes in the NP tissue were observed within 1 to 3 months postoperatively, with an adequate number of cells mainly composed of notochordal cells and chondrocytes, arranged neatly, and a clear demarcation between the NP and the inner AF, with a normal structure of the AF.

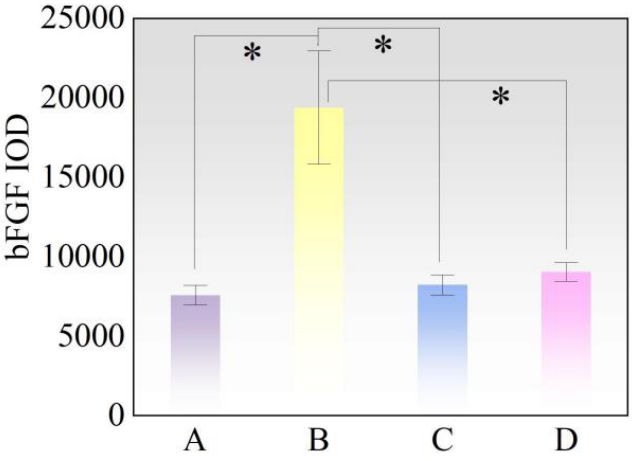

Fig. 1. Immunohistochemical detection of bFGF. (Note: * represents compared to BG, $P < 0.05$).

(2) Control group: Over time, the number of notochordal cells and chondrocytes in the NP gradually decreased from 1 to 3 months postoperatively, the cell distribution became uneven, and some cells aggregated in clusters. The demarcation between the NP and the AF became indistinct, the arrangement of the AF was disordered, and a tendency towards fibrosis appeared.

(3) CG and DG: Within 1 to 3 months postoperatively, the number of NP cells decreased, the cell arrangement was no longer uniform, and the structure of the outer AF was irregular. No clear distinctions in pathological changes were observed between CG and DG.

bFGF immunohistochemical detection

There was an obvious distinction in the IOD of positive cells between AG and BG; The IOD distinction between BG and CG, DG had statistical significance ($P < 0.05$). However, the IOD distinction between AG and CG, DG was not obvious ($P > 0.05$) (Fig. 1).

MMP-13 immunohistochemical detection

The IOD of positive cells had an obvious distinction between AG and BG; The IOD distinction between BG and CG, DG was statistically significant ($P < 0.05$). However, the IOD distinction between AG and CG, DG was not pronounced ($P > 0.05$) (Fig. 2).

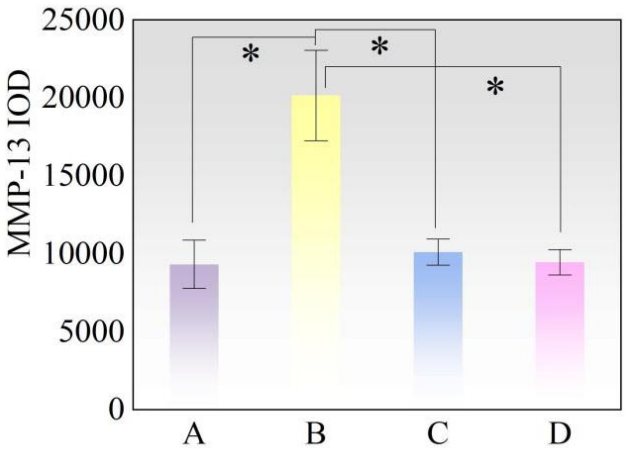

Fig. 2. MMP-13 immunohistochemical detection. (Note: * as against BG, $P < 0.05$).

Correlation between bFGF and MMP-13

The correlation analysis between bFGF and MMP-13 protein expression in NP tissue of BG suggested an obvious correlation ($r = 0.981$, $P < 0.001$) (Fig. 3).

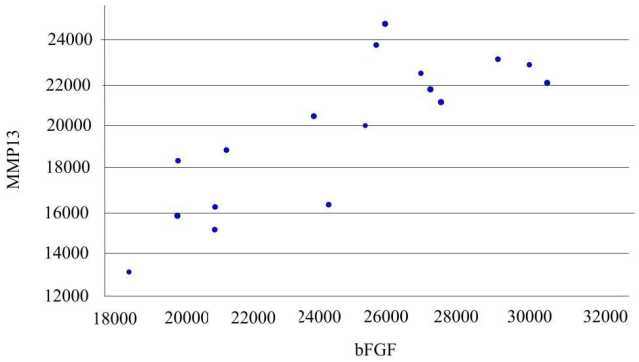

Fig. 3. Correlation between bFGF and MMP-13.

bFGF WB detection

The WB analysis of bFGF indicated a clear distinction between AG and BG; The distinction between BG and CG, DG were statistically significant (P <0.05), but the distinction between AG and CG, DG was not pronounced (P > 0.05) (Fig. 4).

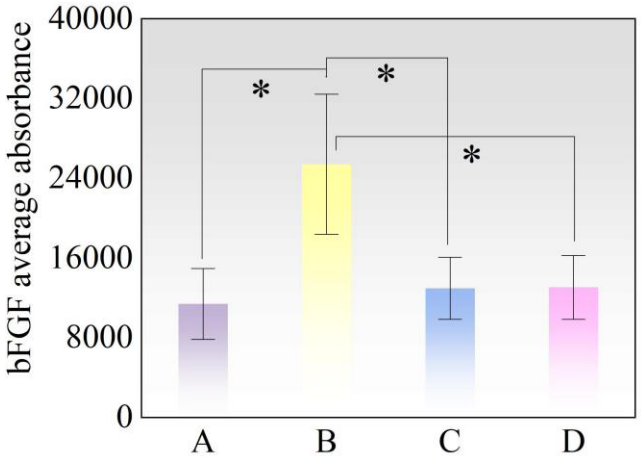

Fig. 4. bFGF WB detection. (Note: * as against BG, $P < 0.05$).

3.6 MMP-13 WB detection

Distinct differences in the WB analysis of MMP-13 were noted between AG and BG; the differences between BG and CG, DG were statistically apparent (P <0.05). No discernible differences were identified between AG and CG, DG ($P > 0.05$) (Fig. 5).

Correlation between bFGF and MMP-13

The correlation analysis between bFGF and MMP-13 protein expression in NP tissue of BG suggested a visible correlation ($r = 0.813$, $P < 0.001$) (Fig. 6).

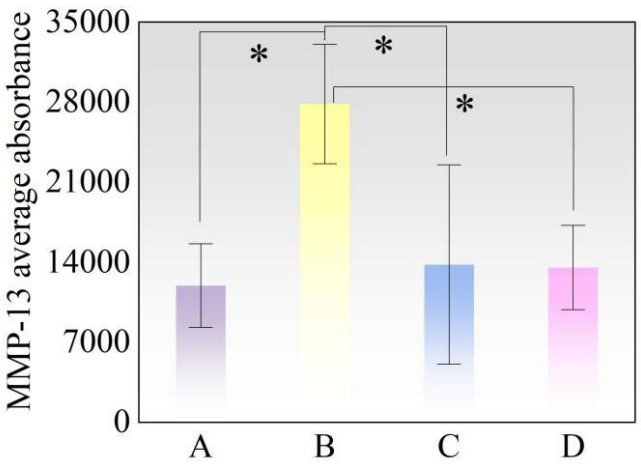

Fig. 5. MMP-13 WB detection. (Note: * as against BG, $P < 0.05$).

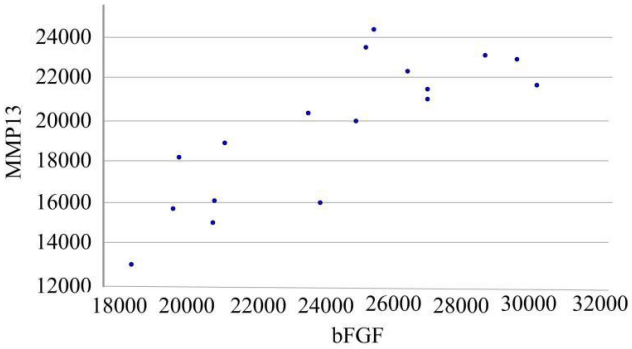

Fig. 6. Correlation between bFGF and MMP-13.

DISCUSSION

For CG and DG, the light microscope observations from HE staining suggested a reduction in the number of cells in the NP tissue, with the cells no longer being evenly arranged, and the structure of the AF was no longer regular. This was similar to the control group, indicating that although Cel could slow down some of the degenerative process, it did not fully restore or maintain the original tissue morphology at the tissue structure level. Additionally, the distinctions between CG and DG were not visible, suggesting that the impact of Cel on tissue morphology at these two dosages was similar.

For bFGF and MMP-13, in BG, the expression levels of these two proteins were markedly higher than in AG, indicating that the upregulation of bFGF and MMP-13 during the process of IVDD may be closely related to the progression of tissue degeneration. The expression of bFGF and MMP-13 in the Cel-treated groups was markedly lower than in BG, indicating that Cel may slow down the degenerative process of the NP tissue by suppressing the expression of these two proteins. It was noted that the IOD

distinctions of bFGF and MMP-13 between AG and CG, DG were not visible, suggesting that the effect of Cel in normal tissue without degeneration was relatively limited. In contrast, in BG, where degeneration had occurred, the inhibitory effect of Cel on bFGF and MMP-13 was more pronounced, which may be related to the drug's regulation of inflammation and extracellular matrix (ECM) degradation processes in pathological states.

The studies by Liu *et al*. (2019b) focused on the development of a tissue engineering substitute for the treatment of IVDD. By using decellularized anulus fibrosus matrix (DAFM) and chitosan mixed hydrogels, combined with bFGF, they constructed a scaffold that simulates the natural tissue structure and mechanical properties. They found that bFGF could promote the proliferation of anulus fibrosus stem cells and the synthesis of anulus fibrosus-related tissues, which, compared with this article, jointly illustrate the dual role of bFGF in the health and degeneration of IVD tissue: in normal or engineered environments, bFGF helps with tissue repair and regeneration; while in degenerated states, overexpression of bFGF may accelerate the degenerative process of the tissue. Therefore, the regulation of bFGF may be an important strategy for the treatment of IVDD, further verifying how the role of bFGF affects the health of IVD tissue in different pathological states.

The studies by Kushioka *et al*. (2019) mainly focused on establishing an efficient culture method for mouse NP cells (mNPCs). Through primary 3D collagen gel culture, mNPCs exhibited morphology and gene expression similar to native NP cells. The experiment found that bFGF gene expression characteristics gradually disappeared in long-term passage culture. The results of this article meant the upregulation of bFGF during the process of IVDD. These two studies jointly illustrate the dual role of bFGF in IVD cells: On the one hand, it can promote the proliferation of NP cells and the synthesis of related tissues, which is of positive significance for tissue engineering and regenerative medicine; on the other hand, in pathological states, overexpression of bFGF may promote the progression of IVDD. Therefore, the regulation of bFGF is not only crucial in cell culture and tissue engineering but also of great significance in disease treatment and degeneration inhibition. In BG, the relationship analysis between bFGF and MMP-13 suggested that there was a visible positive relationship. This indicates that bFGF and MMP-13 may act synergistically in the same pathological mechanism of IVDD. bFGF is usually involved in cell proliferation and matrix synthesis, while MMP-13 is related to matrix degradation, and their co-upregulation may promote abnormal tissue remodeling and degenerative processes of the IVD. The experimental results above show that Cel at different dosages can effectively inhibit the overexpression of bFGF and MMP-13, which may be one of its important mechanisms for slowing down IVDD. Cel, as a selective COX-2 inhibitor, mainly exerts anti-inflammatory effects by suppressing the synthesis of prostaglandins. During the process of IVDD, the occurrence of inflammatory reactions is often accompanied by the upregulation of bFGF and MMP-13, and the anti-inflammatory effect of Cel may reduce the release of inflammatory mediators, thereby indirectly lowering the expression levels of bFGF and MMP-13. In addition, the inhibitory effect of Cel on MMP-13 may also involve its direct regulatory effect on MMP. MMP-13 is mainly responsible for the degradation of matrix components in IVDD, leading to the destruction of the structure of the AF and NP. Cel can protect the structural integrity of the IVD to some extent by suppressing the expression of MMP-13, thus slowing down the degenerative process.

From the results of the WB analysis, the expression of bFGF and MMP-13 was markedly upregulated during the process of IVDD, which may be closely related to the degeneration of the NP tissue and the degradation of the ECM. However, when comparing CG and DG, it was found that the expression levels of bFGF and MMP-13 in both groups were not markedly different from AG ($P > 0.05$), but markedly lower than BG ($P < 0.05$). This suggests that Cel, regardless of the dosage, has an inhibitory effect on the overexpression of these two proteins. Moreover, the distinction between CG and DG was not visible, which may imply that under the current experimental conditions, the effect of Cel has reached a certain saturation state, and further increasing the dosage may not markedly enhance its inhibitory effect. Jhun *et al*. (2022) explored the outcome of vitamin D (VD) in osteoarthritis (OA). Using a monosodium iodoacetate (MIA)-induced rat OA model, the study indicated that the alleviating effect of VD on synovitis. This is somewhat similar to the experimental results of this article, both indicating that in degenerative diseases, the upregulation of inflammatory factors such as MMP-13 is a key factor in tissue degeneration, and suppressing the expression of these factors can effectively slow down the progression of the disease. The relationship analysis of bFGF and MMP-13 in BG suggested a visible positive relationship. The experimental results also suggested that the distinction between CG and DG was not visible, and it was speculated that further increasing the dosage might not bring more visible effects, which may be related to the absorption, distribution, and metabolism of the drug in the tissue. bFGF and MMP-13 were markedly correlated in the degenerative process, indicating that they might play a role in the same pathological pathway. Cel, by suppressing the expression of bFGF, may have indirectly affected the upregulation of MMP-13, thereby suppressing the degeneration of the IVD at multiple levels.

In summary, Cel at different dosages can effectively inhibit the expression of bFGF and MMP-13, which may be achieved by suppressing inflammatory reactions, protecting the ECM, and suppressing the expression of degeneration-related proteins. Although the distinction between CG and DG was not visible, this result suggests the complexity of the dose effect of Cel in the treatment of IVDD. Future studies can further explore the mechanisms of its dose effects and evaluate the safety and efficacy of its long-term use.

CONCLUSION

In this article, an IVDD model was established in SD rats, and methods such as WB were used to systematically evaluate the impact of various doses of Cel on bFGF and MMP-13 in the NP tissue of the IVD. The results suggested that over time, there was a visible reduction in the number of cells and fibrous changes in the NP tissue of BG, while the Cel treatment groups slowed down these pathological changes to some extent. In addition, it was found that CG and DG were both able to effectively inhibit the overexpression of the above two proteins, which was markedly lower as against BG. The results of PCA suggested a visible positive relationship between the expression of bFGF and MMP-13 during the degeneration process, suggesting that they may act synergistically in the same pathological pathway of IVDD. Overall, Cel demonstrated visible anti-degeneration effects in this article, and its mechanism may include suppressing inflammatory responses, protecting the ECM, and suppressing the overexpression of bFGF and MMP-13. Although the therapeutic effects between CG and DG were not markedly different, the potential role of Cel in the treatment of IVDD still warrants further research to optimize its treatment regimen and improve clinical efficacy.

Conflict of Interest. All authors declare they have no conflicts of interest.

Ethics Statement. All animal procedures followed ethical guidelines, with efforts to minimize discomfort and the number of animals used, as approved by the institutional review board.

HU, K.; GAO, H. & WANG, X. Efecto de diferentes dosis de celecoxib en la expresión del factor de crecimiento básico de fibroblastos y la metaloproteinasa de matriz-13 como indicadores morfológicos en un modelo de rata de degeneración del disco lumbar. *Int. J. Morphol., 43(1)*:250-257, 2025.

RESUMEN: El objetivo de este estudio fue investigar los resultados de varias dosis de celecoxib (Cel) en la expresión del factor de crecimiento básico de fibroblastos (bFGF) y la metaloproteinasa de matriz-13 (MMP-13) en un modelo de rata de degeneración del disco intervertebral (IVDD) y su correlación. Se estableció el modelo de rata de IVDD y 68 ratas modeladas con éxito se agruparon: grupos A, B, C y D (AG, BG, CG, DG), con 17 ratas en cada uno. Los cambios patológicos del tejido del núcleo pulposo (NP) y la expresión de bFGF y MMP-13 se detectaron utilizando tinción de hematoxilina-eosina (HE), inmunohistoquímica y transferencia Western (WB), seguido de análisis de correlación de Pearson (PCA). La tinción de HE sugirió que la degeneración del tejido del NP en BG fue clara, y CG y DG desaceleraron hasta cierto punto los cambios patológicos . Los resultados de la inmunohistoquímica y el análisis WB indicaron que la expresión de bFGF y MMP-13 en BG fue notablemente mayor en comparación con AG, y la expresión en CG y DG se redujo notablemente ($P < 0,05$). El coeficiente de correlación de bFGF y MMP-13 en el análisis inmunohistoquímico fue $r = 0,981$ ($P < 0,001$), y en el análisis WB, fue $r = 0,813$ ($P < 0,001$). Se descubrió que Cel inhibe eficazmente la expresión de bFGF y MMP-13 durante el proceso de IVDD, ralentiza el proceso degenerativo y sugiere posibles efectos terapéuticos.

PALABRAS CLAVE: Cel; Degeneración del disco lumbar; bFGF; MMP-13; Análisis de correlación.

REFERENCES

Antonen, E. G.; Kruchek, M. M. & Nikitina, M. V. Evaluation of the effectiveness of treatment of patients with nonspecific pain syndrome in the lower back with celecoxib and a combined preparation of B vitamins. *Zh. Nevrol. Psikhiatr. Im. S. S. Korsakova., 122(8)*:65-72.

Bouhsina, N.; Tur, L.; Hardel, J. B.; Madec, S.; Rouleau, D.; Etienne, F.; Guicheux, J.; Clouet, J. & Fusellier, M. Variable flip angle T1 mapping and multi-echo T2 and T2* mapping magnetic resonance imaging sequences allow quantitative assessment of canine lumbar disc degeneration. *Vet. Radiol. Ultrasound, 64(5)*:864-72.

Chang, Y. C.; Lin, C. W.; Chang, Y. S.; Chen, P. H.; Li, C. Y.; Wu, W. C. & Kao, Y. H. Monounsaturated oleic acid modulates autophagy flux and upregulates angiogenic factor production in human retinal pigment epithelial ARPE-19 cells. *Life Sci., 259*:118391, 2020.

Hu, L.; Luo, D.; Zhang, H. & He, L. Polydatin inhibits IL-1b-mediated chondrocyte inflammation and ameliorates cartilage degradation: Involvement of the NF-kB and Wnt/b-catenin pathways. *Tissue Cell.,78*: 101865, 2022.

James, J. J.; Sandhya, K. V.; Sridhar, K. N.; Sudarson, S.; Basavaraj, B. V. & Bharath, S. Proteomic characterization of human placenta: insights into potential therapeutic applications for osteoarthritis. A*APS PharmSciTech., 25(6)*:139, 2024.

Jhun, J.; Woo, J. S.; Kwon, J. Y.; Na, H. S.; Cho, K. H.; Kim, S. A.; Kim, S. J.; Moon, S. J.; Park, S. H. & Cho, M. L. Vitamin D attenuates pain and cartilage destruction in OA animals via enhancing autophagic flux and attenuating inflammatory cell death. *Immune. Netw., 22(4)*:e34, 2022.

Kasamkattil, J.; Gryadunova, A.; Schmid, R.; Gay-Dujak, M. H. P.; Dasen, B.; Hilpert, M.; Pelttari, K.; Martin, I.; Schären, S.; Barbero, A.; Krupkova, O. & Mehrkens, A. Human 3D nucleus pulposus microtissue model to evaluate the potential of pre-conditioned nasal chondrocytes for the repair of degenerated intervertebral disc. *Front Bioeng. Biotechnol., 11*:1119009, 2023.

Kim, J. H.; Ham, C. H. & Kwon, W. K. Current knowledge and future therapeutic prospects in symptomatic intervertebral disc degeneration. *Yonsei Med. J., 63(3)*:199-210, 2022.

Kirnaz, S.; Capadona, C.; Wong, T.; Goldberg, J. L.; Medary, B.; Sommer, F.; McGrath, L. B. Jr. & Härtl, R. Fundamentals of intervertebral disc degeneration. *World Neurosurg., 157*: 264-73, 2022.

Kushioka, J.; Kaito, T.; Chijimatsu, R.; Okada, R.; Ishiguro, H.; Bal, Z.; Kodama, J.; Takenaka, S.; Makino, T.; Sakai, Y. & Yoshikawa, H. A novel and efficient method for culturing mouse nucleus pulposus cells. *Spine J., 19(9)*:1573-83, 20219.

Li, Q.; Ding, F. & Liu, X. L. Research progress in nucleus pulposus tissue engineering in lumbar intervertebral disc. *Zhongguo Yi Xue Ke Xue Yuan Xue Bao, 46(1)*:88-97, 2024.

Liu, C.; Jin, Z.; Ge, X.; Zhang, Y. & Xu, H. Decellularized annulus fibrosus matrix/chitosan hybrid hydrogels with basic fibroblast growth factor for annulus fibrosus tissue engineering. *Tissue Eng. Part A, 25(23-24)*:1605-13, 2019a.

Liu, H. & Li, Y. Potential roles of cornichon family AMPA receptor auxiliary protein 4 (CNIH4) in head and neck squamous cell carcinoma. *Cancer Biomark., 35(4)*:439-50, 2022.

Liu, H. & Tang, T. A bioinformatic study of IGFBPs in glioma regarding their diagnostic, prognostic, and therapeutic prediction value. *Am. J. Transl. Res., 15(3)*:2140-55, 2023.

Liu, P.; Gu, L.; Ren, L.; Chen, J.; Li, T.; Wang, X.; Yang, J.; Chen, C. & Sun, L. Intra-articular injection of etoricoxib-loaded PLGA-PEG-PLGA triblock copolymeric nanoparticles attenuates osteoarthritis progression. *Am. J. Transl. Res., 11(11)*:6775-89, 2019b.

Ma, M.; Ma, G.; Zhang, C.; Wang, Y.; He, X. & Kang, X. Identification of autophagy-related genes involved in intervertebral disc degeneration by microarray data analysis. *World Neurosurg., 188*:e1-e17, 2024.

Payet, M.; Ah-Pine, F.; Guillot, X. & Gasque, P. Inflammatory mesenchymal stem cells express abundant membrane-bound and soluble forms of C-Type lectin-like CD248. *Int. J. Mol. Sci., 24(11)*:9546, 2023.

Rabie, M. A.; Sayed, R. H.; Venkatesan, J. K.; Madry, H.; Cucchiarini, M. & El Sayed, N. S. Intra-articular injection of rAAV-hFGF-2 ameliorates monosodium iodoacetate-induced osteoarthritis in rats via inhibiting TLR-4 signaling and activating TIMP-1. *Toxicol. Appl. Pharmacol., 459*:116361, 2023.

Sun, K.; Zhu, L. G.; Wei, X.; Yin, H.; Zhan, J. W.; Yin, X. L. & Han, T. Research progress in mechanism of Chinese herbal compounds and monomers in delaying lumbar intervertebral disc degeneration. *Zhongguo Zhong Yao Za Zhi, 47(9)*:2400-8, 2022.

Wang, Y.; Zhang, Z.; Wang, L.; Wang, H. & Dong, F. Rare NUP98::PRRX1 fusion transcript in a therapy-related acute myeloid leukemia associated with del(7q) following chemotherapy for diffuse large B-cell lymphoma. *Cancer Genet., 284-285*:12-15, 2024.

Xu, G.; Zhang, C.; Zhu, K.; Ye, Y. & Bao, Z. Effects of lentivirus-mediated insulin-like growth factor 1 and platelet derived growth factor genes on nucleus pulposus tissue of human degenerated intervertebral disc. *Zhongguo Xiu Fu Chong Jian Wai Ke Za Zhi, 34(7)*:907-914, 2020.

Xu, J.; Song, J.; Zhu, W.; Zuo, L.; Wu, J.; Zhang, L.; Wang, T. & Guo, J. A novel germline frameshift mutation in the MLH1 gene in a patient with Lynch syndrome. *Cancer Genet., 274-275*:54-58, 2023.

Zhu, D.; Miao, Z.; Dong, M.; Lin, J.; Wang, Y.; Tian, N.; Luo, P.; Lin, Y.; Wu, Y. & Chen, M. Development of a novel rat intervertebral disc degeneration model by surgical multifidus resection-induced instability. *World Neurosurg., 165*: e357-e364, 2022.

Corresponding author:
Xueli Wang
Department of Radiology
The First Affiliated Hospital of Xi'an Medical University
Xi'an 710077
Shaanxi Province
CHINA

E-mail: wang780304@163.com